

**Supplemental Materials for:**  
**Infrared spectroscopy study of the in-plane response of  $\text{YBa}_2\text{Cu}_3\text{O}_{6.6}$**   
**in magnetic fields up to 30 Tesla**

F. Lyzwa<sup>1</sup>, B. Xu<sup>1</sup>, P. Marsik<sup>1</sup>, E. Sheveleva<sup>1</sup>, I. Crassee<sup>2</sup>, M. Orlita<sup>2</sup>, C. Bernhard<sup>1</sup>

<sup>1</sup>*University of Fribourg, Department of Physics and Fribourg Center for Nanomaterials, Chemin du Musée 3, CH-1700 Fribourg, Switzerland*

<sup>2</sup>*Laboratoire National des Champs Magnétiques Intenses (LNCMI), CNRS-UGA-UPS-INSA, 25, Avenue des Martyrs, 38042 Grenoble, France*

**I. Magnetization measurements to determine  $T_c$**

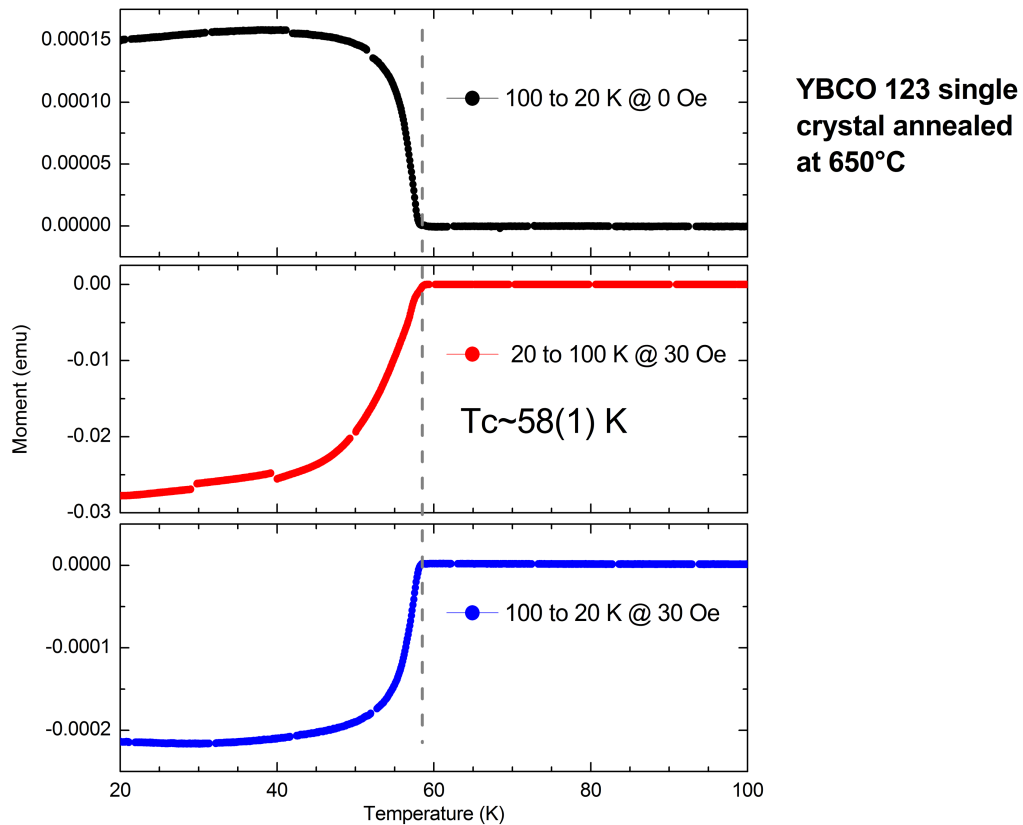


**Figure 1.** Vibration sample measurement (VSM) performed with a Quantum Design PPMS device. For the underdoped  $\text{YBa}_2\text{Cu}_3\text{O}_{6.6}$  crystal its superconducting transition temperature was determined to be  $T_c = 58(1)$  K.

## II. Correction of the c-axis contribution and temperature-dependent shift of the plasma edge

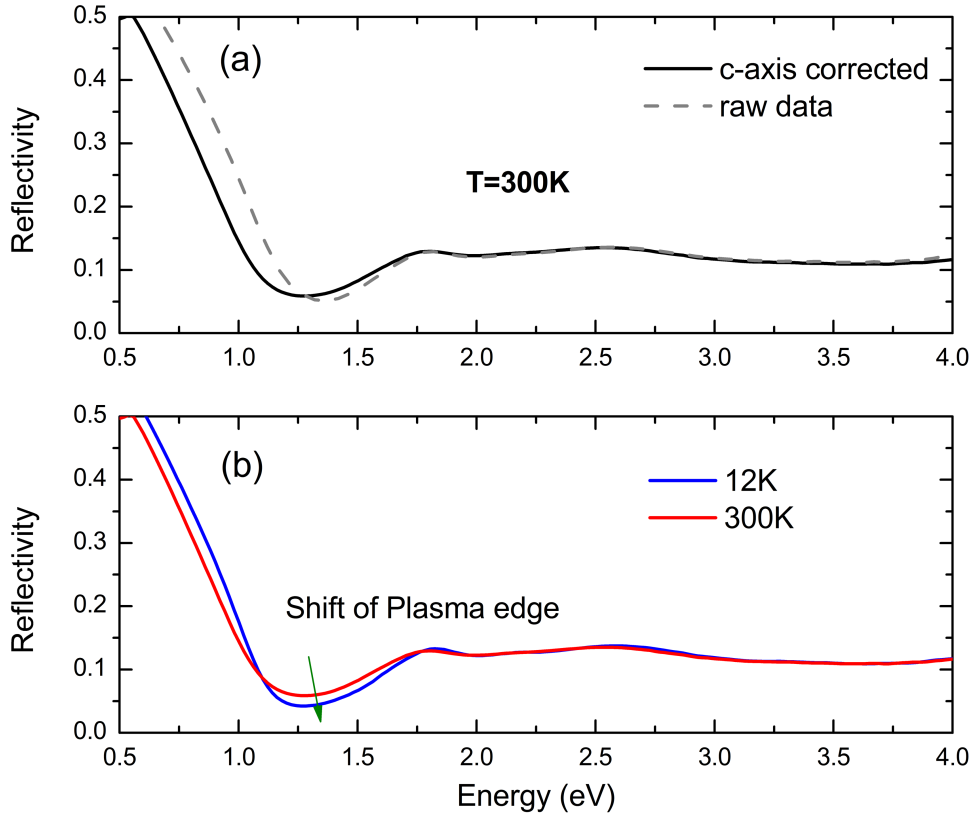


**Figure 2.** Visible to near-infrared reflectivity spectra of the YBa<sub>2</sub>Cu<sub>3</sub>O<sub>6.6</sub> crystal. **(a)** By measuring the reflectivity at an angle of incidence  $\phi > 0$ , we are not only probing the in-plane ( $ab$ -plane) response of the sample, but also some contribution from the out-of-plane ( $c$ -axis) response. This can be corrected by measuring the  $c$ -axis component and applying a simple thin film model. **(b)** The plasma edge shifts to higher energies by going from 300 K to 12 K due to the stronger Drude response [1].

### III. Magneto-optical measurements

The magnetic field dependent measurements of the  $\text{YBa}_2\text{Cu}_3\text{O}_{6.6}$  crystal were performed via a Bruker VERTEX 80v Fourier transform infrared spectrometer being attached to a long pipe (to ensure, that the optical components inside the spectrometer chamber get not affected by the magnetic field), which is connected to a beam splitter (BS) (see Fig. 3).

The sample was placed in a sealed volume with low-pressure helium exchange gas that was inserted into a liquid helium bath with  $T=4.2$  K (or in a nitrogen bath with  $T=77$  K) and surrounded by a resistive coil which creates the magnetic field, in a way that  $B$  is parallel to the incoming/outgoing light and perpendicular to the sample surface. In the so-called Faraday configuration, the light  $I_0$  travels from the spectrometer through the pipe to the BS until it hits the sample surface, where it is reflected back to the BS and finally arrives at the Bolometer, where the total reflectivity  $I_r$  is detected.

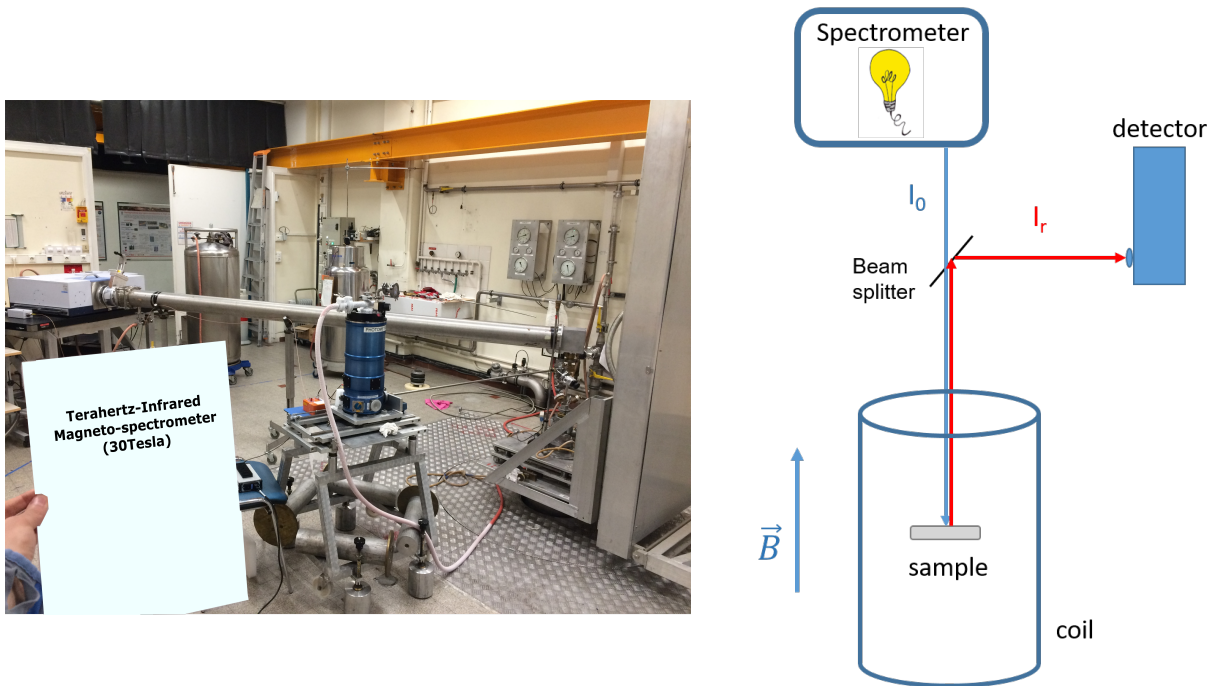


**Figure 3.** Experimental setup for magnetic field dependent reflectivity measurements: Picture (left) and sketch (right).

The magneto-optical measurements on the  $\text{YBa}_2\text{Cu}_3\text{O}_{6.6}$  crystal were always done by referencing to a gold mirror placed in a special holder (see Fig. 4), in order to avoid contribution from the setup itself. Since the B-field was applied while the sample being already in the superconducting state, the strong repulsion forces were acting on the crystal and causing a movement. To avoid this sample movement, we fixed the sample with an additional holder piece from the backside.

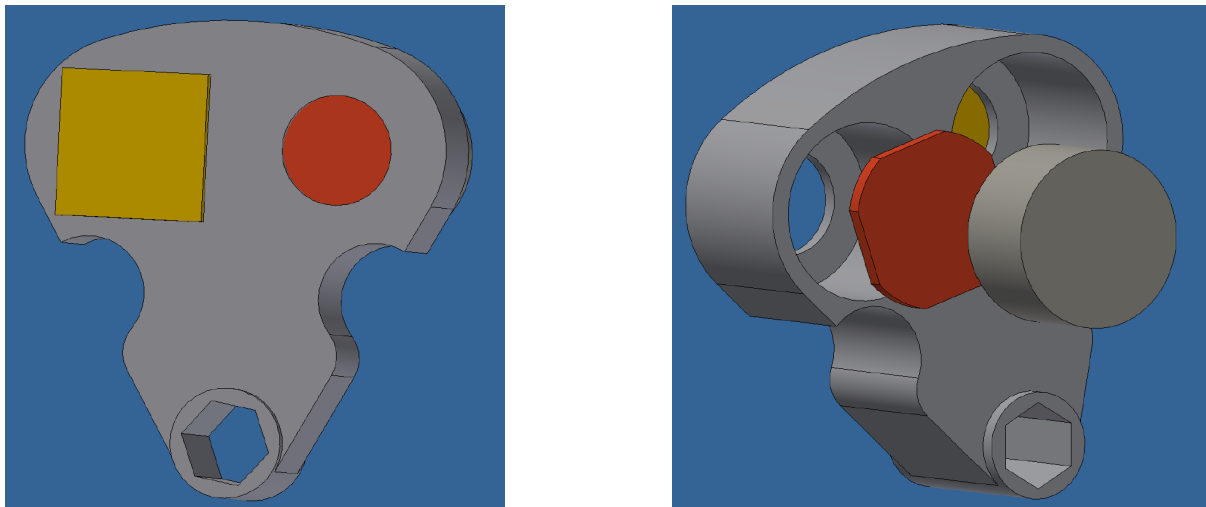


**Figure 4.** Sample holder configuration for magnetic field measurements. The reference gold mirror (yellow) is fixed from the frontside of the holder (left image), whereas the  $\text{YBa}_2\text{Cu}_3\text{O}_{6.6}$  crystal (red) is fixed with an additional holder piece from the backside (right image).



#### IV. Magnetic-field-induced changes in the low-energy spectra

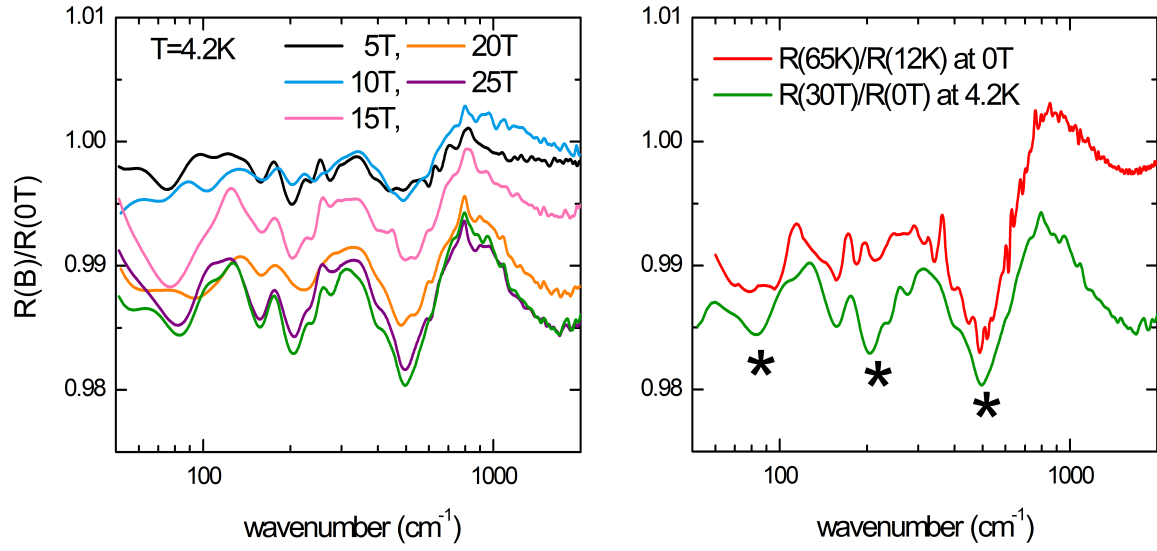


**Figure 5.** Enlarged view of Fig 2(a), (c) in the manuscript, showing several reflectivity ratios for the low-energy part of the spectra. Left panel: Evolution of the spectra for different magnetic fields applied (B || c-axis). Right panel: Magnetic field (green) and temperature (red) effect are compared to each other. The stars label the two enhanced electronic modes (at 240  $\text{cm}^{-1}$  and 90  $\text{cm}^{-1}$ ) and as well as the dip around 500  $\text{cm}^{-1}$ , which is attributed to the suppression of the SC condensate.

## V. Impact of the choice of the extrapolation to higher energies

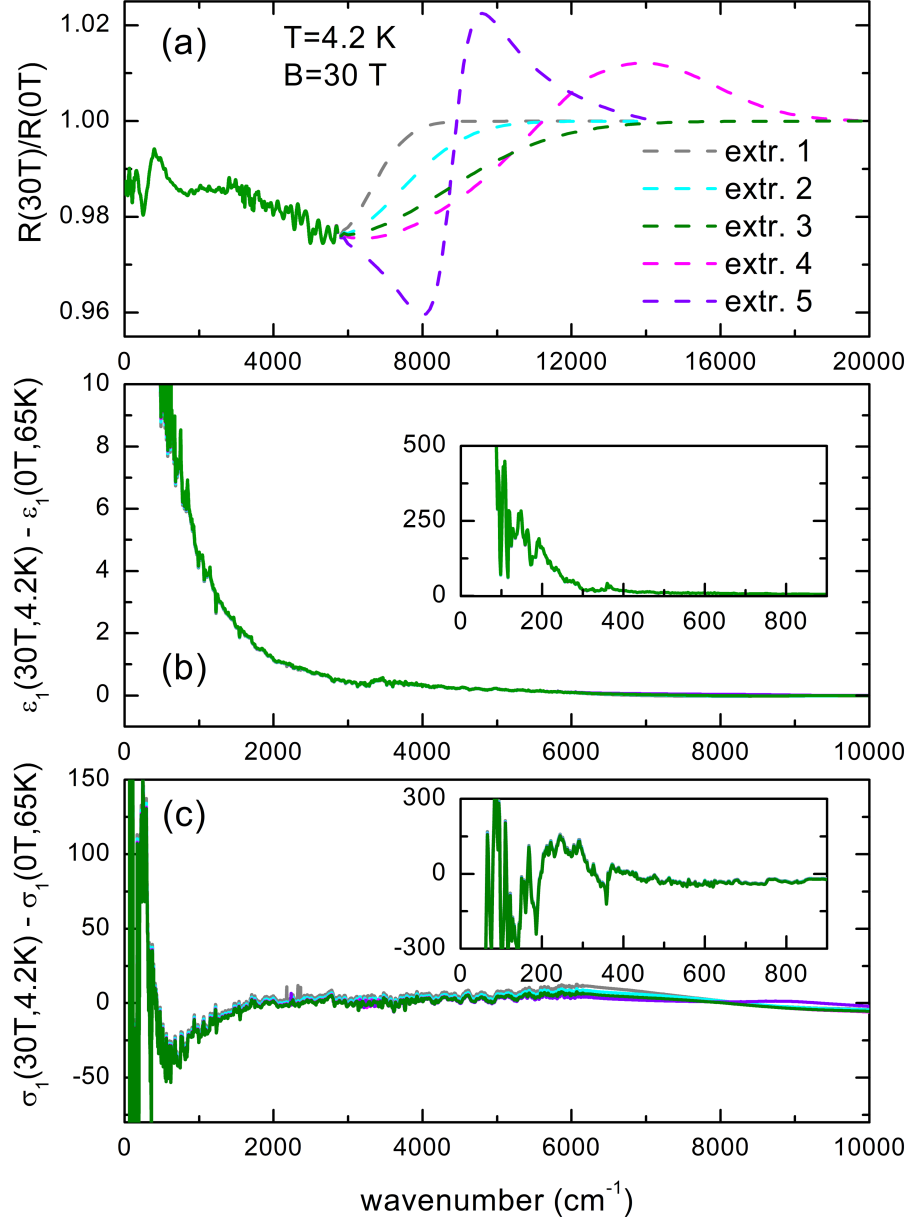


**Figure 6. (a)** Possible extrapolations for the high-energy side of the magnetic field dependent data. In order to perform a Kramers-Kronig transformation, we assumed that the off-diagonal terms of the dielectric function tensor are relatively small and can therefore be neglected. **(b)** and **(c)**: The choice of the extrapolation do not lead to significant differences for the low energy region of the spectra, as can be seen in the difference plots  $\Delta\epsilon_1$  and  $\Delta\sigma_1$ . For the maindraft, we chose extrapolation type 3. It presents the most simplistic assumption, that the reflectivity curve (when  $B=30$  Tesla applied) smoothly approaches the one for zero-field.

## References

- [1] A. V. Boris, N. N. Kovaleva, O. V. Dolgov, T. Holden, C. T. Lin, B. Keimer and C. Bernhard, "In-Plane Spectral Weight Shift of Charge Carriers in  $\text{YBa}_2\text{Cu}_3\text{O}_{6.9}$ ," *Science*, vol. 304, pp. 708-710, 2004.